

1 Alkalinity sources in the Dutch Wadden Sea

2 Mona Norbistrath^{1,2,3}, Justus E. E. van Beusekom¹, & Helmuth Thomas^{1,2}

3 ¹Institute of Carbon Cycles, Helmholtz-Zentrum Hereon, Geesthacht, 21502, Germany

4 ²Institute for Chemistry and Biology of the Marine Environment (ICBM), Carl von Ossietzky University Oldenburg,
5 Oldenburg, 26129, Germany

6 ³now at: Department of Marine Chemistry and Geochemistry, Woods Hole Oceanographic Institution, Woods Hole, MA,
7 02543, USA

8 *Correspondence to:* Mona Norbistrath (mona.norbistrath@whoi.edu)

9 Abstract

10 Total alkalinity (TA) is an important chemical property playing a decisive role in the oceanic buffering capacity of CO₂. TA
11 is mainly generated by weathering on land, and by various anaerobic metabolic processes in water and sediments. The Wadden
12 Sea, located in the southern North Sea is hypothesized to be a source of TA for the North Sea, but quantifications are scarce.
13 This study shows observations of TA, dissolved inorganic carbon (DIC), and nutrients in the Dutch Wadden Sea in May 2019.
14 Along several transects, surface samples were taken to investigate spatial distribution patterns and to compare them with data
15 from the late 1980s. A tidal cycle was sampled to further shed light on TA generation and potential TA sources. We identified
16 the Dutch Wadden Sea as a source of TA with an average TA generation of 7.6 μmol TA kg⁻¹ h⁻¹ during ebb tide in the Ameland
17 Inlet. TA was generated in the sediments with deep pore water flow during low tide enriching the surface water. A combination
18 of anaerobic processes and CaCO₃ dissolution were potential sources of TA in the sediments. We deduce that seasonality and
19 the associated nitrate availability in particular influence TA generation by denitrification, which is low in spring and summer.

20 1 Introduction

21 As the regulator of the ocean carbon dioxide (CO₂) sink, total alkalinity (TA) is of increasing scientific interest and is
22 investigated worldwide in the so called “Anthropocene” (Abril and Frankignoulle, 2001;Bozec et al., 2005;Chen and Wang,
23 1999;Dickson, 1981;Middelburg et al., 2020;Norbistrath et al., 2022;Renforth and Henderson, 2017;Thomas et al.,
24 2004;2009;Sabine et al., 2004). The “Anthropocene” describes the current era of our planet, when environmental changes,
25 driven by humans, have become identifiable in geological records (Zalasiewicz et al., 2010;Crutzen, 2002). One of the most
26 threatening changes for our climate is the anthropogenic driven increase in atmospheric greenhouse gases (GHG), such as
27 CO₂. To counteract the increasing atmospheric CO₂ concentrations and the ongoing climate warming, a combination of several
28 pathways is needed. Beside a strict reduction of CO₂ emissions, also net-negative emissions are required, which capture the
29 atmospheric CO₂ and store it either based on land or in the ocean (e.g., Keith et al., 2006;Matthews and Caldeira, 2008;Zhang

30 et al., 2022). The climate and the increasing atmospheric CO₂ content is also naturally regulated by the open ocean, and around
31 a quarter of the global anthropogenic CO₂ emissions are already removed by it (Friedlingstein et al., 2022). The carbon storage
32 capacity of the North Sea is an important atmospheric CO₂ sink as it exports the absorbed CO₂ in the deep layers of the Atlantic
33 Ocean where it is stored on longer time scales (Borges et al., 2005;Bozec et al., 2005;Burt et al., 2016;Brenner et al., 2016;Hu
34 and Cai, 2011;Schwichtenberg et al., 2020;Thomas et al., 2004;2009). Two important aspects of the oceanic climate regulation
35 are the oceanic circulation and TA. TA, primarily consisting of bicarbonate and carbonate, is generated by chemical rock
36 weathering (Suchet and Probst, 1993;Meybeck, 1987;Berner et al., 1983), and in various stoichiometries by calcium carbonate
37 (CaCO₃) dissolution and anaerobic metabolic processes, such as denitrification, which is the reduction process of nitrate to
38 dinitrogen gas in the nitrogen cycle (Hu and Cai, 2011;Wolf-Gladrow et al., 2007;Chen and Wang, 1999;Brewer and Goldman,
39 1976). Since TA, CO₂ uptake and its export to the deep ocean are mainly disentangled in the open ocean, TA and the oceanic
40 circulation interact closely in highly active and shallow ocean areas such coastal zones and continental and marginal shelves.
41 In these shallow areas, TA is susceptible to changes due to various metabolic processes and the influence of adjacent zones
42 like rivers, estuaries, marshes, and tidal flats (e.g., Norbistrath et al., 2022;2023;Wang et al., 2016;Voynova et al., 2019). A
43 previous study by Norbistrath et al. (2022) showed that an enhanced riverine, metabolic alkalinity would lead to increasing
44 CO₂ absorption in the coastal zones of the North Sea, highlighting the need to further investigate TA regulation in adjacent
45 zones of coastal oceans.

46 Coastal zones, which are the direct interface between most, if not all, compartments of the Earth system (i.e., atmospheric,
47 terrestrial, aquatic, and oceanic) and human societies, appear particularly vulnerable to environmental and climate change
48 (Glavovic et al., 2015). This holds true for the Wadden Sea, the shallow, coastal sea along an approximately 500 km coastline
49 of the Netherlands, Germany, and Denmark, in the southern North Sea, which is declared as an UNESCO world natural heritage
50 site since 2009. Most of the Wadden Sea is located between the protecting barrier Islands and the Mainland, which makes it
51 the world's largest uninterrupted stretch of tidal flats with multiple tidal inlets (Fig. 1). Due to the topography, the Wadden
52 Sea is a highly dynamic ecosystem with influences from the mainland and the North Sea (Hoppema, 1993;Postma, 1954;van
53 Raaphorst and van der Veer, 1990). Driving forces of the biogeochemical dynamics in the Wadden Sea are nutrient imports
54 by rivers and high suspended particulate matter (SPM) and organic matter (OM) imports from the North Sea (van Beusekom
55 et al., 2019;van Beusekom et al., 2012;Postma, 1954). Physical sources of variability in the Wadden Sea are oceanic driven
56 wind, waves, and tidal currents, as well as the counterclockwise circulation of the North Sea (Elias et al., 2012). Large tidal
57 amplitude and currents in conjunction with shallow water depths allow for vertical water column mixing and an exchange
58 between the pelagic and benthic realms including deep pore water exchange (Røy et al., 2008). The strong tidal currents also
59 impact the biogeochemistry of the North Sea (Postma, 1954), as they cause an exchange of water between the North Sea and
60 the Wadden Sea and play an important role in the import of particulate matter from the North Sea (Burchard et al., 2008).
61 Previous studies identified the Wadden Sea as a TA source for the North Sea with a loading between 39 Gmol yr⁻¹
62 (Schwichtenberg et al., 2020) and 73 Gmol yr⁻¹ (Thomas et al., 2009). Both studies suggested the entire Wadden Sea as one of
63 the most important TA sources of the carbon storage capacity for the North Sea. Burt et al. (2016) highlighted the importance

64 of coastal TA production for regulating the buffer system in the North Sea, and suggested denitrification as the major TA
65 source. Due to the strong connection between the North Sea and the Wadden Sea, a better understanding of TA generation in
66 the latter is required. Here, we focus on the Dutch Wadden Sea that has been well-studied during the past decades (Hoppema,
67 1990, 1991, 1993;De Jonge et al., 1993;Elias et al., 2012;Ridderinkhof et al., 1990;Postma, 1954;van Beusekom et al.,
68 2019;Schwichtenberg et al., 2017). In particular Hoppema (1990);(1993) observed the spatial and temporal variability of TA
69 in May in the late 1980s, which we compare with our observed transect data to detect potential differences over the last 30
70 years. In addition, we further discussed potential TA sources in the Dutch Wadden Sea.

71 **2 Methods**

72 **2.1 Study site and sampling**

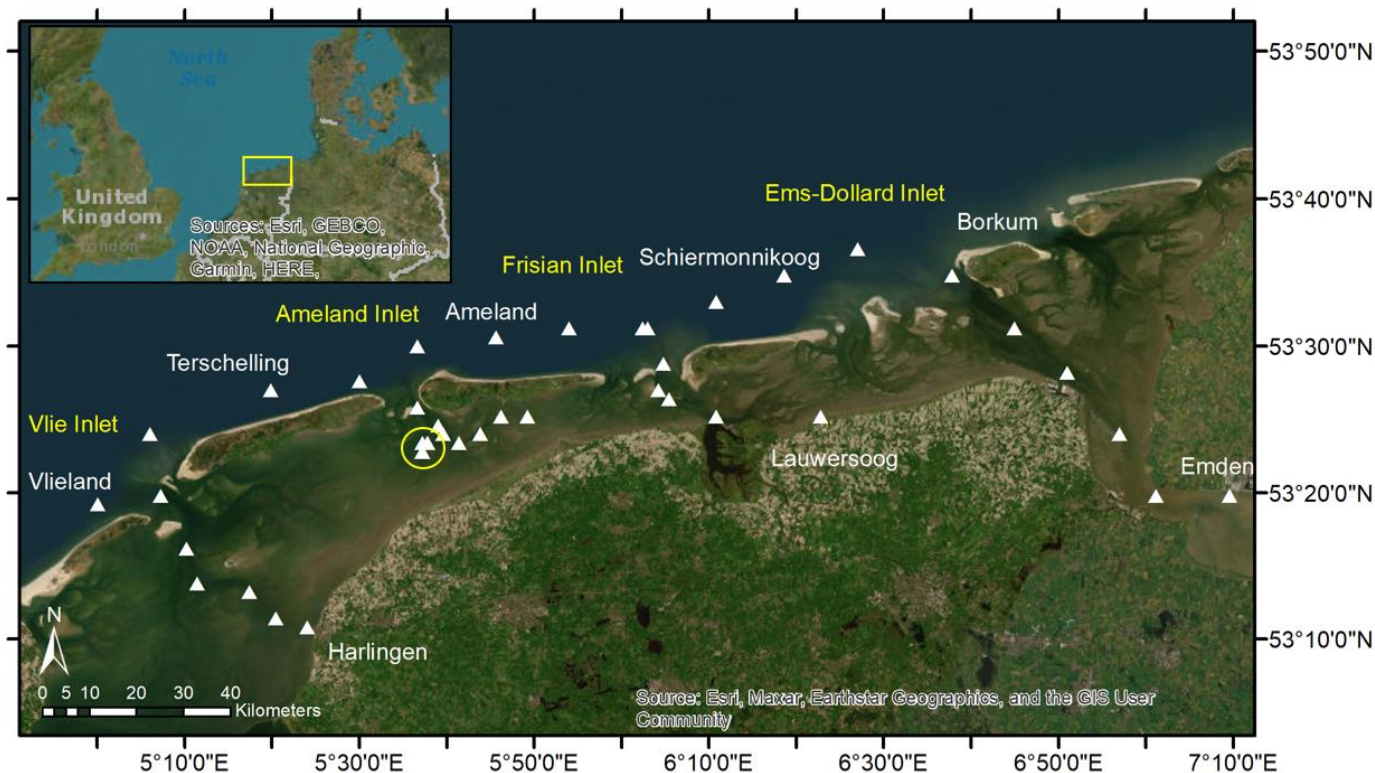
73 This study is based on samples collected on a research cruise (LP20190515) in the Dutch Wadden Sea (Frisian Islands) on RV
74 *Ludwig Prandtl* in May 2019 (Fig. 1). We collected water samples in the Wadden Sea starting at Harlingen, through the Vlie
75 Inlet along the islands Vlieland and Terschelling, through the Ameland Inlet to Ameland Island, from there on via the Frisian
76 Inlet to Lauwersoog, and around Schiermonnikoog Island via the Ems-Dollard Inlet to Emden. In addition, we sampled a half
77 tidal cycle during ebb tide (from high tide to low tide) on 21 May 2019. To set the range of ebb tide data in relation, we also
78 sampled a half tidal cycle during flood tide (from low tide to high tide) on 23 May 2019 for comparison. Both half tidal cycles
79 were sampled as an anchor station in the waterway at the western side of Ameland in the Ameland Inlet on each day.

80 Nearly half-hourly, we collected discrete surface (1.2 m depth) water samples with a bypass from the onboard flow-through
81 FerryBox system (Petersen et al., 2011), which also provided essential physical parameters such as salinity and temperature.

82 For TA and DIC measurements we sampled water with overflow into 300 mL BOD (biological oxygen demand) bottles and
83 preserved them with 300 μ L saturated mercury chloride solution (HgCl_2) to stop biological activity. Each BOD bottle was
84 filled without air bubbles and closed by using a ground-glass stopper coated in Apiezon® type M grease and a plastic cap. The
85 samples were stored in a cool dark environment until measurements in the lab.

86 Water for nutrient samples was filtered through pre-combusted (4 h, 450 °C) GF/F filters and the filtrate was stored frozen in
87 three 15 mL Falcon tubes for triplicate measurements in the lab.

88 To determine the total carbon (C), organic carbon (C_{org}) and nitrogen (N) concentrations in SPM and associated $C_{\text{org}}:\text{N}$ ratios,
89 we used pre-combusted (4 h, 450 °C) GF/F filters, which were dried after sampling at 50 °C to remove all humidity and were
90 stored frozen afterwards until measurement.



91
 92 **Figure 1** Sampling site in the Dutch Wadden Sea. The sampling stations around the Frisian Islands in May 2019 are visualized
 93 with white triangles. The yellow circle highlights the anchor stations for the tidal cycle sampling in the Ameland Inlet on two
 94 days. During the sampling day from low tide to high tide, we had two samples that we took slightly more western due to
 95 drifting. The island and city names are shown in white, the inlets in yellow. The tidal flats and sedimentary structures are well
 96 visible between the barrier islands and the mainland.

97 **2.2 Carbon species analyses**

98 The parallel analyses of TA and DIC were carried out in March 2020 by using the VINDTA 3C (Versatile INSTRument for the
 99 Determination of Total dissolved inorganic carbon and Alkalinity, MARIANDA - marine analytics and data), which measures
 100 TA by potentiometric titration and DIC by coulometric titration both with a measurement precision $< 2 \mu\text{mol kg}^{-1}$ (Shadwick
 101 et al., 2011). Certified reference material (CRM batch # 187) provided by Andrew G. Dickson (Scripps Institution of
 102 Oceanography) was measured before and after the samples and used to ensure a consistent calibration of both measurements.
 103 The calcite and aragonite saturation states (Ω) and the pH were computed with the CO₂SYs program (Lewis and Wallace,
 104 1998), using the measured parameters TA, DIC, salinity, temperature, silicate and phosphate as input variables, together with
 105 the dissociation constants from Mehrbach et al. (1973), as refit by Dickson and Millero (1987).

106 **2.3 Nutrient analyses**

107 The nutrients were measured with a continuous flow automated nutrient analyzer (AA3, SEAL Analytical) and a standard
108 colorimetric technique (Hansen and Koroleff, 2007) for nitrate (NO_3^-), nitrite (NO_2^-), phosphate (PO_4^{3-}), and silicate (Si), and
109 a fluorometric method (K  rouel and Aminot, 1997) for ammonium (NH_4^+) (Grasshoff et al., 2009). The nutrient samples were
110 measured against reference materials VKI SW4.1B (NO_x , NO_2 and NH_4) and VKI SW4.2B (Si and PO_4) in July 2019. The
111 maximum standard deviations were $0.322 \mu\text{mol L}^{-1}$ for NO_3^- , $0.014 \mu\text{mol L}^{-1}$ for NO_2^- , $0.081 \mu\text{mol L}^{-1}$ for NH_4^+ , $0.014 \mu\text{mol}$
112 L^{-1} for PO_4^{3-} and $0.165 \mu\text{mol L}^{-1}$ for Si.

113 For the C_{org} determination, filters were acidified with 1N HCl and dried overnight to remove all inorganic carbon content.
114 Filters were measured with a CHN-elemental analyzer (Eurovector EA 3000, HEKAtech GmbH) in the Institute of Geology,
115 University Hamburg, and calibrated against a certified acetanilide standard (IVA Analysentechnik, Germany). The standard
116 deviations were 0.05 % for carbon and 0.005 % for nitrogen.

117 **2.4 Data analyses**

118 The data analyses were performed by using RStudio Version 1.3.1073    2009-2020 RStudio, PBC. The linear regression
119 Model II was performed by using the “lmodel2” R package, and the plots were created with the “ggplot2” R package.

120 **3 Results**

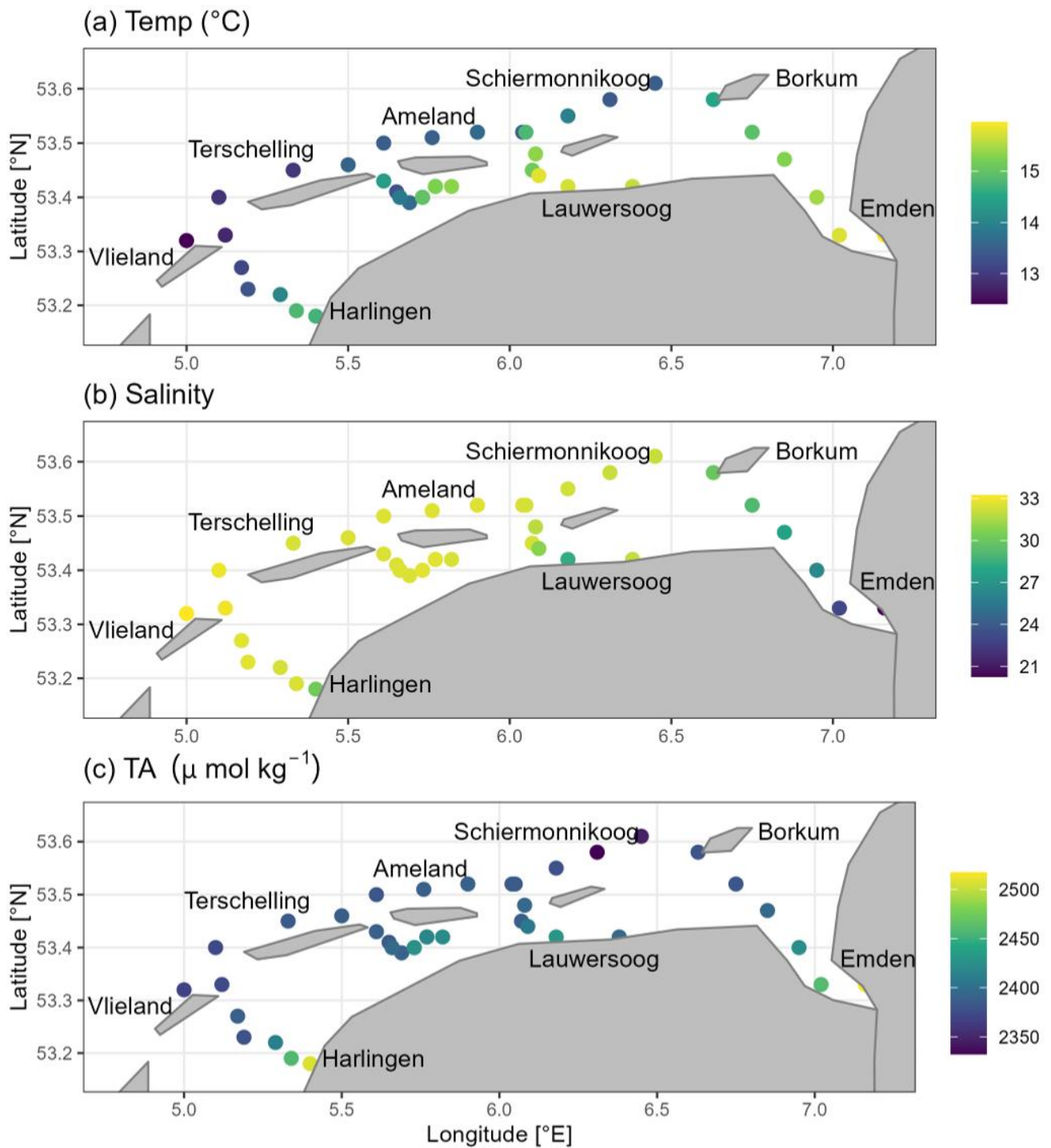
121 **3.1 Spatial parameter distribution**

122 To investigate the spatial distribution of TA in the Dutch Wadden Sea and compare its general status with earlier studies (in
123 particular Hoppema, 1990), we observed TA and related parameters in surface water along a transect from the coastal mainland
124 towards the North Sea.

125 The temperatures varied between 12 and 16   C with higher temperatures towards the coastal mainland (Fig. 2a). We identified
126 two main sub regions based on the salinity values. First the Ems-Dollard Inlet, which showed salinities lower than 28 and with
127 the minimum value of 20.25 at the most upstream station. And second, around Ameland Island and the remaining of our
128 investigated region in the Dutch Wadden Sea with salinities showing only minor differences varying from 28 to 33 (Fig. 2b).
129 Spatial transect TA concentrations ranged from $2332 \mu\text{mol TA kg}^{-1}$ to $2517 \mu\text{mol TA kg}^{-1}$. We observed lower concentrations
130 on the North Sea side of the Frisian Islands with somewhat higher concentrations around Ameland (Fig. 2c). In contrast to the
131 North Sea side, the values were higher ($> 2380 \mu\text{mol TA kg}^{-1}$) in the Wadden Sea. In the Ems-Dollard Inlet, the concentrations
132 were even higher, with values up to $2517 \mu\text{mol TA kg}^{-1}$ at the most upstream station.

133 Silicate (Si) showed higher concentrations in the Wadden Sea and lower ones towards the North Sea (Fig. A1a). Highest
134 concentrations were observed at the coastal mainland and in the Ems-Dollard Inlet. Silicate concentrations ranged between 0.3
135 and $56.3 \mu\text{mol Si L}^{-1}$. Both, the calcite and aragonite saturation states (Ω) were supersaturated in the entire study region.

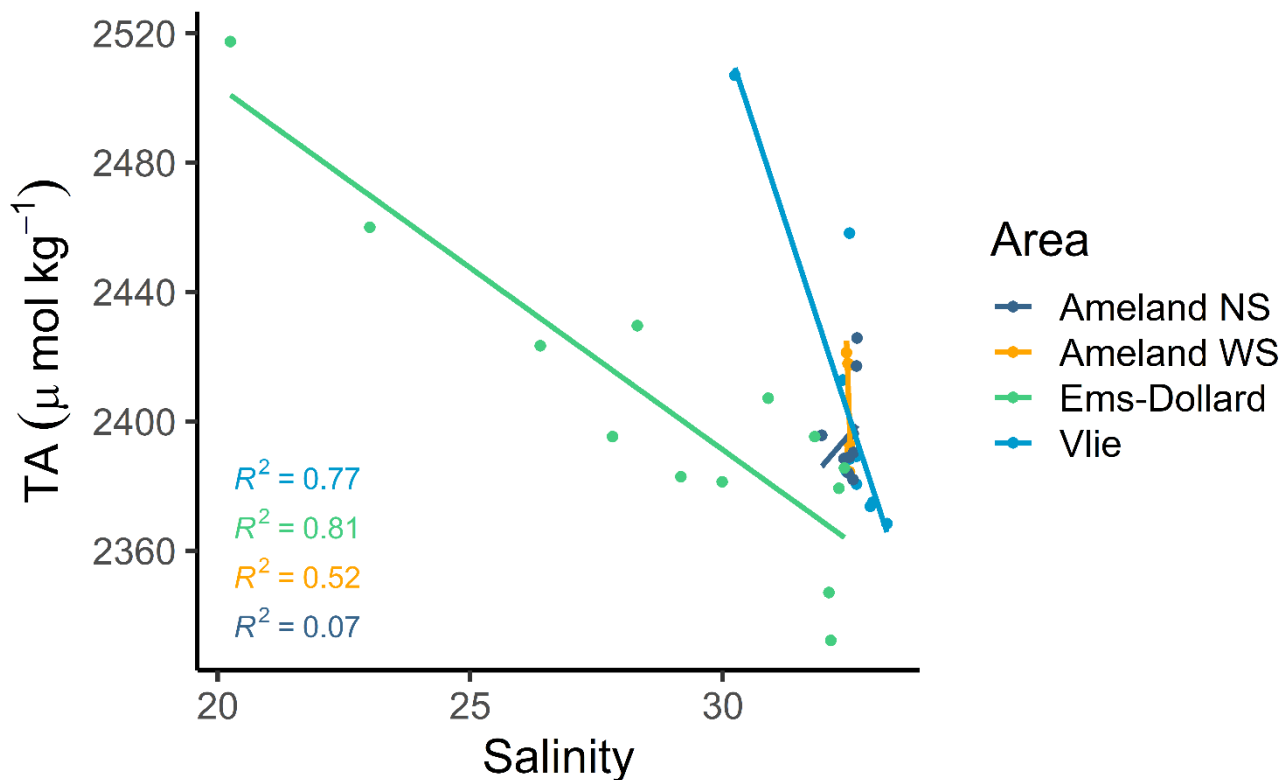
136 Saturation state values ranged from 2.3 to 4.6 for calcite (Fig. A1b), and from 1.4 to 3.0 for aragonite (Table B1). Highest
137 values were observed at the North Sea side of the barrier islands, and lowest values near Harlingen and in the Ems-Dollard
138 Inlet. Like the calcite and aragonite saturation states, the pH values were higher in the North Sea, and lower in the Wadden
139 Sea and near the coastal mainland (Fig. A1c). The pH values ranged from 7.86 to 8.19, and lowest values were observed near
140 Harlingen and in the Ems-Dollard Inlet. The nitrate (NO_3^-) concentrations were in a low range ($< 3 \mu\text{mol NO}_3^- \text{ L}^{-1}$) throughout
141 the study region. Higher concentrations ($< 6 \mu\text{mol NO}_3^- \text{ L}^{-1}$) were observed only at a few stations close to land, and maximum
142 concentrations ($< 38 \mu\text{mol NO}_3^- \text{ L}^{-1}$) were observed in the Ems-Dollard Inlet (Fig. A1d). DIC concentrations ranged from 2097
143 $\mu\text{mol DIC kg}^{-1}$ to 2430 $\mu\text{mol DIC kg}^{-1}$ (Fig. A1e). DIC values showed a similar pattern as TA values, with higher concentrations
144 near the coastal mainland and in the Ems-Dollard Inlet, and decreasing concentrations toward the North Sea, where DIC
145 reached minimum values.



146

147 **Figure 2** Spatial distribution of a) temperature ($^{\circ}\text{C}$), b) salinity, and c) total alkalinity (TA; $\mu\text{mol kg}^{-1}$) from surface water
 148 samples in May 2019.

149 Compared to the other transects of this study region, the strong influence of the inner Ems Estuary is visible at the most
150 upstream station in the Ems-Dollard Inlet, showing lowest pH and calcite saturation state values, and highest values of TA,
151 DIC, nitrate, silicate and phosphate. The outer side of the Vlie Inlet reflects the North Sea conditions with lower temperatures
152 and higher salinities. The North Sea impact is also visible in the mixing plot between TA and salinity (Fig. 3). Statistical
153 significant linear mixing behavior was observed in the transect through the Ems-Dollard Inlet ($R^2 = 0.81$) and through the Vlie
154 Inlet ($R^2 = 0.77$), where TA concentrations decreased with increasing salinities from the mainland towards the North Sea (Fig.
155 3). Whereas in the Ems-Dollard Inlet mixing is dominated by riverine water with high TA concentrations, the mixing in the
156 Vlie Inlet showed a more prominent mixing of Wadden Sea and North Sea water. The TA concentrations in the Vlie Inlet and
157 around Ameland, both at the North Sea side (Ameland NS) and the Wadden Sea side (Ameland WS) were higher than the TA
158 concentration computed for the salinity end-member in the Ems-Dollard Inlet, suggesting the Dutch Wadden Sea as a source
159 of TA (Fig. 3). Both the Ameland NS and WS data clearly indicated a non-conservative behavior with a range of TA
160 concentrations at near constant salinities.



162 **Figure 3** Mixing plot of total alkalinity (TA) and salinity in the North Sea side of Ameland and the Frisian Inlet (Ameland
163 NS), in the Wadden Sea site of Ameland (Ameland WS), around Schiermonnikoog and in the Ems-Dollard Inlet (Ems-
164 Dollard), and in the Vlie Inlet (Vlie).

165 **3.2 Tidal cycle**

166 We observed a half tidal cycle at an anchor station in the Ameland Inlet during ebb tide, to 1) identify potential TA sources
167 and 2) to quantify potential TA export to the North Sea. We identified patterns in several biogeochemical parameters in water
168 leaving the tidal flats (Fig. 4, Table B1). Temperature increased from 13.25 to 14.7 °C (Fig. 4a). Salinity was constant around
169 32.5(Fig. 4b, Table B1), which is in the range of southern North Sea water excluding admixture of local fresh water sources.
170 During ebb tide, TA ranged from 2387 $\mu\text{mol TA kg}^{-1}$ during high tide to 2438 $\mu\text{mol TA kg}^{-1}$ during low tide (Fig. 4c). We
171 observed an increase of 51.6 $\mu\text{mol TA kg}^{-1}$ (ΔTA) during ebb tide (6.8 h), resulting in a TA increase of 7.6 $\mu\text{mol TA kg}^{-1} \text{ h}^{-1}$
172 at the sampling location.

173 DIC concentrations behaved similar to TA with minimum values at high tide (2172 $\mu\text{mol DIC kg}^{-1}$), and maximum values
174 (2273 $\mu\text{mol DIC kg}^{-1}$) at low tide, resulting in an increase of 101.3 $\mu\text{mol DIC kg}^{-1}$ (ΔDIC) or 14.9 $\mu\text{mol DIC kg}^{-1} \text{ h}^{-1}$ (Fig. 4d).
175 DIC increased almost twice as much as TA.

176 Nitrate increased during ebb tide by 0.92 $\mu\text{mol NO}_3^- \text{ L}^{-1}$ (ΔNO_3^-) from a minimum of 1.26 $\mu\text{mol NO}_3^- \text{ L}^{-1}$ to a maximum of
177 2.17 $\mu\text{mol NO}_3^- \text{ L}^{-1}$ (Fig. 4e), resulting in a nitrate increase of 0.13 $\mu\text{mol NO}_3^- \text{ L}^{-1} \text{ h}^{-1}$.

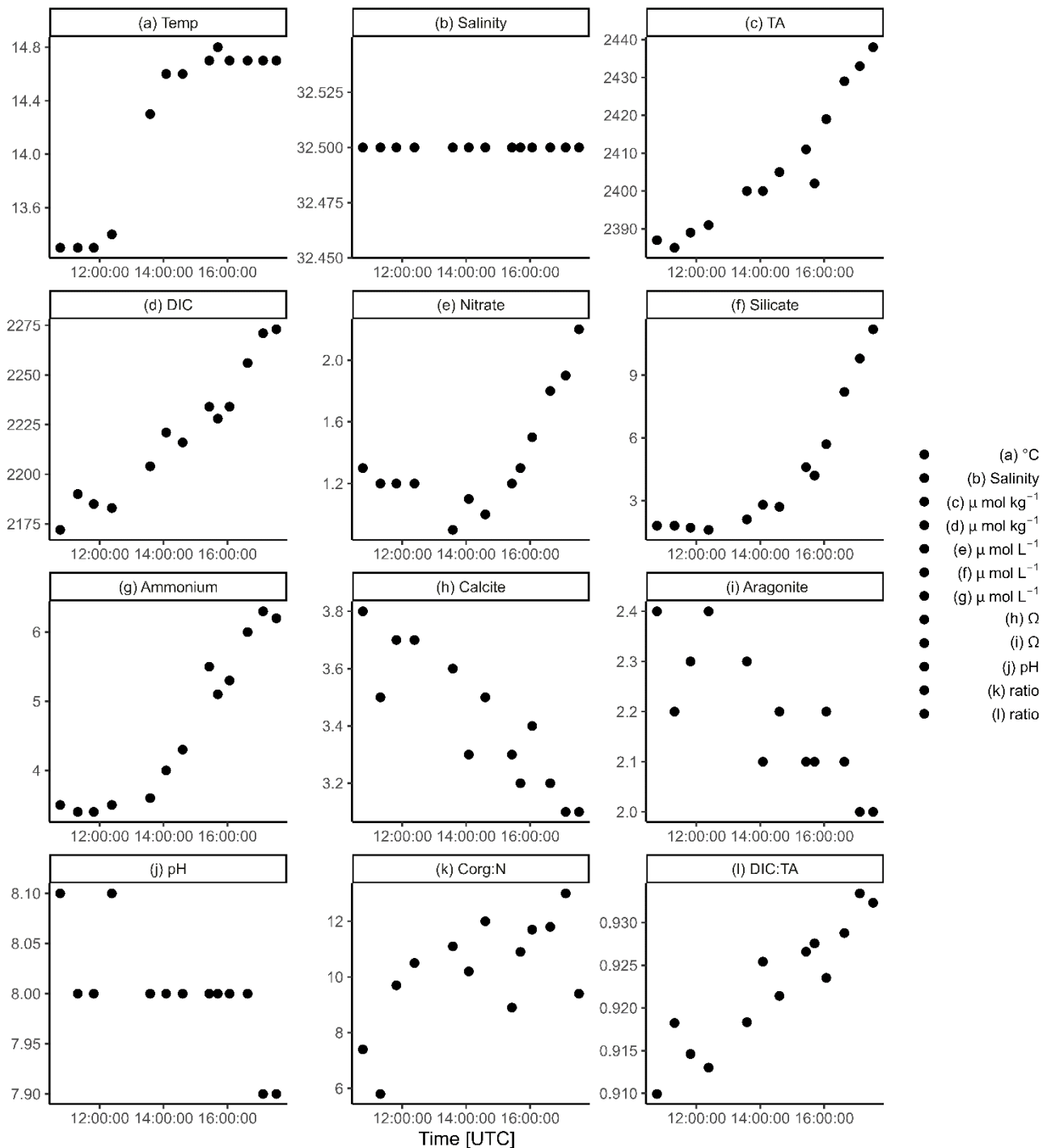
178 Silicate showed a similar pattern with low values (1.8 $\mu\text{mol Si L}^{-1}$) at high tide increasing during ebb tide to a maximum of
179 11.2 $\mu\text{mol Si L}^{-1}$, resulting in a silicate increase (ΔSi) of 9.4 $\mu\text{mol Si L}^{-1}$ or 1.4 $\mu\text{mol Si L}^{-1} \text{ h}^{-1}$ during ebb tide (Fig. 4f).

180 Ammonium increased from 3.47 $\mu\text{mol NH}_4^+ \text{ L}^{-1}$ to 6.22 $\mu\text{mol NH}_4^+ \text{ L}^{-1}$ during ebb tide (Fig. 4g), resulting in an ammonium
181 increase (ΔNH_4^+) of 2.74 $\mu\text{mol NH}_4^+ \text{ L}^{-1}$, or 0.4 $\mu\text{mol NH}_4^+ \text{ L}^{-1} \text{ h}^{-1}$.

182 The calcite and aragonite saturation states had maximum values ($\Omega_{\text{Ca}} = 3.8$, $\Omega_{\text{Ar}} = 2.4$) at high tide and decreased to their
183 minimum ($\Omega_{\text{Ca}} = 3.1$, $\Omega_{\text{Ar}} = 2.0$) during ebb tide (Fig. 4h,i). The influence of the North Sea is indicated by the observed
184 maximum at high tide, which decreased during the ebb.

185 Like omega, the maximum pH was 8.07 at high tide and decreased to a minimum (7.93) during ebb tide (Fig. 4j).

186 $\text{C}_{\text{org}}:\text{N}$ ratios of SPM increased during ebb tide (Fig. 4k). A minimum $\text{C}_{\text{org}}:\text{N}$ ratio of 5.6 was observed around high tide and
187 increased to a maximum of 13.0 during ebb tide. Simultaneously, the SPM concentration increased during ebb tide, from 12.8
188 mg SPM L^{-1} to a maximum of 82.4 mg SPM L^{-1} at the second last station (Table B1).



189

190 **Figure 4** A half tidal cycle from high tide to low tide. Temporal distribution of a) temperature, b) salinity, c) total alkalinity
 191 (TA), d) dissolved inorganic carbon (DIC), e) nitrate, f) silicate, g) ammonium, h) calcite saturation state (Ω), i) aragonite

192 saturation state (Ω), j) pH, k) $C_{\text{org}}:\text{N}$ ratio of SPM, and l) DIC:TA ratio. Note the different y-axes and the +1 hour time
193 difference between the local time and the UTC time.

194 3.3 TA generation

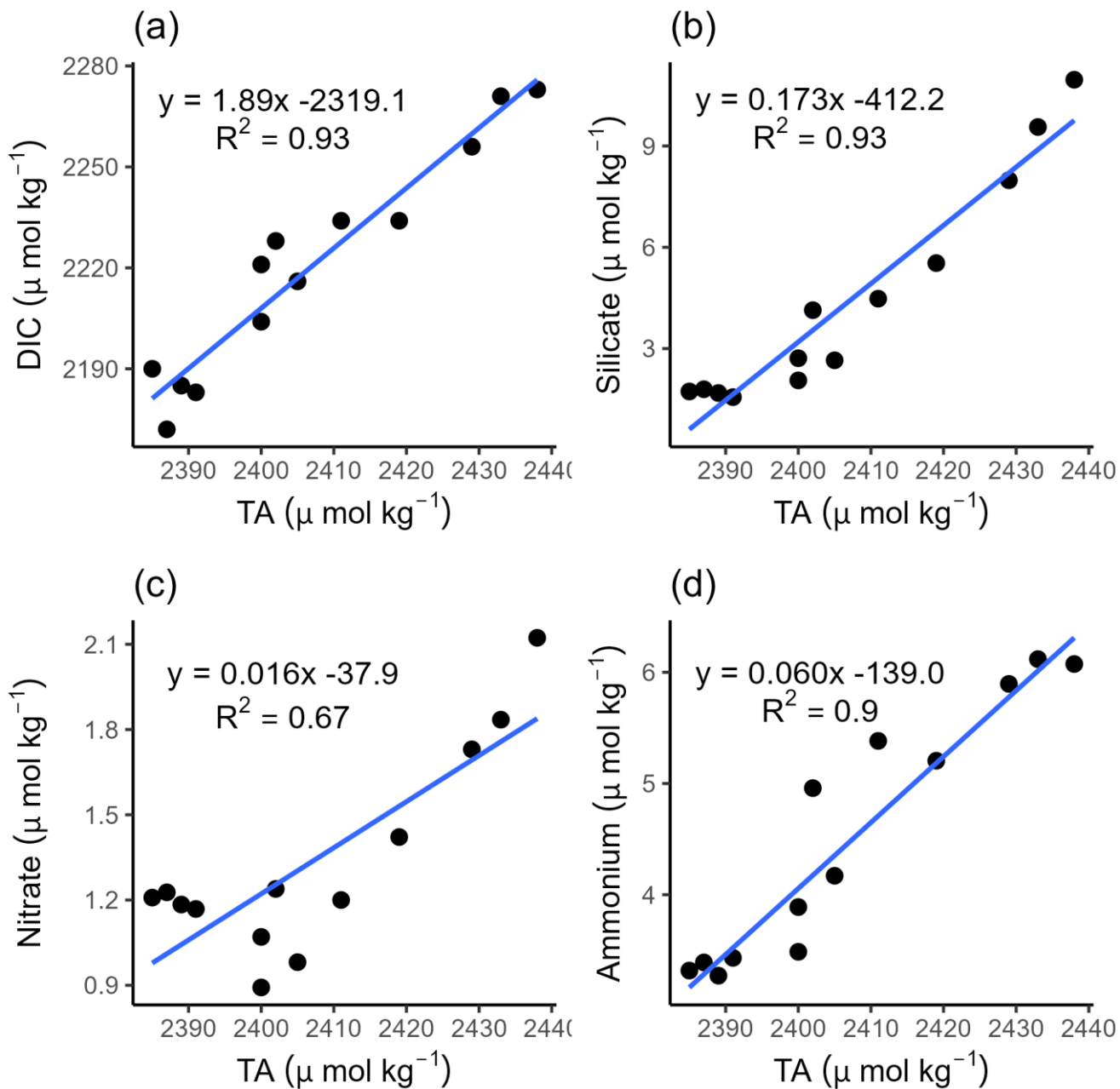
195 Tidal forcing leads to a bi-diurnal exchange between Wadden Sea and North Sea water. The tidal forcing also induces a strong
196 benthic-pelagic coupling (Huettel et al., 2003; Røy et al., 2008). Many studies support that the outflowing water exports
197 material from the sediment including remineralization products from organic matter (e.g., Billerbeck et al., 2006; Røy et al.,
198 2008). Here, we focus on the hypothesis that the sediments are a significant source of TA.

199 For a first rough estimate of a maximum TA export during ebb tide, we used the mean observed TA increase ($\Delta\text{TA} / 2$) of 25.8
200 $\mu\text{mol TA kg}^{-1}$ during ebb tide (in the Ameland Inlet, part of the Borndiep tidal basin), a tidal prism of $478 \cdot 10^6 \text{ m}^3$ of the
201 Borndiep tidal basin, and a share of intertidal flats of 53 % (Louters and Gerritsen, 1994). Assuming that only the intertidal
202 sediments exchange TA, we estimated a TA export of 6.6 Mmol TA per tide to the North Sea. Assuming two ebb tides and a
203 lunar cycle of 24.8 hours this would result in a daily export of 12.7 Mmol TA.

204 The significant correlation of TA and silicate ($R^2 = 0.93$), and the insignificant relation between TA and salinity ($R^2 = 0.32$),
205 as well as silicate and salinity ($R^2 = 0.21$), suggest that TA originates from the tidal flats in this part of the Dutch Wadden Sea
206 and is not from admixture carried by river runoff. The significant correlation between TA and silicate both during ebb tide
207 point to the same source (Fig. 5b).

208 To further elucidate potential TA sources in the Dutch Wadden Sea, we correlated TA with DIC, silicate, nitrate, and
209 ammonium in the half tidal cycle from high tide to low tide, respectively (Fig. 5).

210 The correlation between TA and DIC is a measure between anaerobic and aerobic processes. Our data show a strong positive
211 correlation between DIC and TA ($R^2 = 0.93$) with TA concentrations being higher than DIC concentrations (Fig. 5a). We
212 observed a release excess of DIC compared to TA as indicated by the slope of 1.89 and by an increase in DIC ($\Delta\text{DIC} = 101.3$
213 $\mu\text{mol kg}^{-1}$) almost twice as high as TA ($\Delta\text{TA} = 51.6 \mu\text{mol kg}^{-1}$) (Fig. 5a). This excess DIC may be caused by strong CO_2
214 production due to high aerobic OM degradation, or by uptake from the atmosphere due to water movement by tidal forcing.
215 However, given the heterotrophic nature of the Wadden Sea (e.g., van Beusekom et al., 2012), a CO_2 undersaturation is
216 unlikely. The TA increase can be fueled by various processes which we will discuss below. We detected a linear positive
217 correlation of increasing TA and silicate ($R^2 = 0.93$) during ebb tide, supporting pore water outflow (Fig. 5b) as pore water is
218 the major Si source during summer (van Bennekom et al., 1974). A stronger influence of the pore water with ongoing ebb tide
219 is indicated by increasing values. The positive correlation between nitrate and TA ($R^2 = 0.67$) (Fig. 5c) was less strong than
220 the correlations between TA and DIC, and TA and Si, which could be traced back on an effect of the first four samplings points
221 that were probably at the tipping point from high tide to low tide. In the remaining samples, the increasing nitrate and TA
222 concentrations suggest a stronger TA generation than nitrate production, balancing TA that may be consumed by nitrification
223 (i.e., nitrate production).



224

225 **Figure 5** Correlations of TA with a) dissolved inorganic carbon (DIC), b) silicate, c) nitrate, and d) ammonium during ebb

226 tide in the Ameland Inlet.

227 **4 Discussion**

228 **4.1 Spatial TA variability**

229 Hoppema (1990) reported TA distributions in the westernmost part of the Dutch Wadden Sea around the barrier islands Texel,
230 Vlieland, and Terschelling. He focused on the tidal basins drained by the tidal inlets Marsdiep and Vlie located more to the
231 west than our sampling stations (not visible on the map). Hoppema (1990) did not observe a continuous increase of salinity in
232 the Wadden Sea from the fresh water source towards the North Sea and associated this to the influence of tidal differences and
233 an arbitrary sampling scheme. The presence (dominance) of North Sea water in the Dutch Wadden Sea and on the tidal flats
234 is supported by our transect data, which show relatively high salinities at coastal North Sea level. Brackish salinities were only
235 detected in the large Ems-Dollard Inlet, which receives fresh water from the river Ems, and close to Harlingen and Lauwersoog,
236 which have direct fresh water inflows by smaller rivers and streams. The absence of clear salinity gradients in the more eastern
237 part of the Dutch Wadden Sea investigated in our study suggest that most of the IJsselmeer discharge was exchanged with the
238 North Sea through the Marsdiep (e.g., Duran-Matute et al., 2014).

239

240 The spatial TA data by Hoppema (1990), show lower TA concentrations at stations with more fresh water influence and higher
241 TA concentrations in the tidal inlets. The data of this study also show high TA concentrations in the tidal inlets, suggesting
242 TA generation in sediments, which is possibly fueled by high imports of nutrients and OM (van Beusekom and De Jonge,
243 2002). The even higher TA concentrations at stations with lower salinities close to the mainland observed in this study also
244 show the influence from the catchment area on the coast, and possibly TA generation in the shallow sediments near the coast.
245 In May (1986), Hoppema (1990) found TA concentrations ranging between 2319 and 2444 $\mu\text{mol TA kg}^{-1}$ at salinities between
246 18.62 and 29.17. Our lowest observed TA concentration was 2332 $\mu\text{mol TA kg}^{-1}$ at a salinity of 32.14, and our highest TA
247 concentration was 2517 $\mu\text{mol TA kg}^{-1}$ at a salinity of 20.25 close to the coastal mainland. A comparison of both studies shows
248 that the general TA levels are in a similar range, but that the spatial gradients are opposite.

249 A conservative mixing between TA and salinity is only visible in the Ems-Dollard Inlet and the Vlie Inlet (Fig. 3). While the
250 conservative mixing in the Ems-Dollard Inlet is more dominated by the fresh water discharge from the Ems River, the
251 conservative mixing in the Vlie Inlet is more dominated by North Sea water passing through this deep inlet and allowing more
252 North Sea water to be transported towards the coast. After the Marsdiep Inlet, the Vlie Inlet has the highest average tidal prism
253 and is the second largest inlet in the Dutch Wadden Sea (Elias et al., 2012). Similar to our findings, Hoppema (1990) noted a
254 linear mixing of TA and salinity in the Vlie Inlet, and suspected a lower fresh water contribution there as well, which is in
255 accordance with model data (Duran-Matute et al., 2014).

256 In the Ems-Dollard Inlet, conservative mixing was observed, indicating minor contributions from other sources. In a previous
257 study, Norbistrath et al. (2023) observed very high TA concentrations and TA generation in the upper tidal river of the highly
258 turbid Ems Estuary, which may explain the high levels of TA in the Ems-Dollard Inlet (at low salinities) observed in this study.

259 Hoppema (1990) also observed a range of TA concentrations in the Dutch Wadden Sea and related these to different sinks and
260 sources. TA sinks can be calcium carbonate (CaCO_3) precipitation, or extraction of seawater carbonate by mollusks (e.g., Chen
261 and Wang, 1999;Hoppema, 1990). Variable fresh water inflows can either serve as a sink or a source (e.g., Chen and Wang,
262 1999;Hoppema, 1990). Other TA sources can be CaCO_3 dissolution, anaerobic metabolic processes in the sediment, or erosion
263 of TA enhancing sediments (e.g., Hoppema, 1990;Chen and Wang, 1999).

264 Except for the Ems-Dollard Inlet and close to Harlingen, we observed mainly marine salinities (> 30) but higher TA values in
265 the Dutch Wadden Sea than in the North Sea. We therefore exclude possible TA sinks and focus only on TA sources. According
266 to Hoppema (1990), the main causes for TA variations in the Dutch Wadden Sea were fresh water inflows and sources in the
267 sediment. In our study, fresh water inflows with high TA concentrations were only observed in the Ems-Dollard Inlet, but not
268 around the islands and the tidal flats. For a further TA source identification in the Dutch Wadden Sea, we investigated the TA
269 variability during ebb tide in a tidal channel close to Ameland.

270 **4.2 Determination of TA generation**

271 Burt et al. (2016) and Schwichtenberg et al. (2020) indicated TA generation in the Wadden Sea as an important source for the
272 North Sea's carbon storage capacity. Here, we want to further identify TA generation and potential TA sources.

273 In a study from the late 1980s, Hoppema (1993) observed a tidal cycle in the Marsdiep in May and September. Focusing on
274 TA, DIC, and oxygen, he also observed increasing TA values during ebb tide and assumed the tidal flats and discharging rivers
275 and canals as TA sources. Comparing our present TA data and the historical TA data, there is not a large difference in the
276 range of values observed during a tidal cycle. However, a further in-depth interpretation and comparison of both TA data sets
277 is limited by the low number of data, leading us to focus on TA generation during our cruise.

278 We made a very rough first estimate of the daily TA export. By using a 3D ecosystem model, Schwichtenberg et al. (2020)
279 estimated an annual export of 10 to 14 Gmol TA yr^{-1} for the entire Dutch Wadden Sea. Given that the Borndiep tidal basin
280 covers about 14% of the Dutch Wadden Sea and assuming no seasonal dynamics, our estimate of 12.7 Mmol d^{-1} compares
281 well with the annual averaged model estimate of 4.6 Mmol TA d^{-1} , but the overestimation suggests that seasonal dynamics
282 may be involved. Since our TA export based only on a half tidal observation, the inclusion of it into the model used by
283 Schwichtenberg et al. (2020) would be unreliable (personal communication J. Pätsch, 2022). To test whether the observed TA
284 generation matches their suggested TA export, observational data of at least each season are required to run the model and
285 gain a representative result (personal communication J. Pätsch, 2022).

286 **4.3 TA source attribution**

287 **4.3.1 Local sediment outwash**

288 In order to gain further insight into potential sources of TA, we compared our TA and nutrient data. The main focus was on
289 dissolved silicate (Si) as van Bennekom et al. (1974) showed that this nutrient is depleted in the Wadden Sea during the spring

290 diatom blooms and further showed that pore water is the main source of dissolved Si during summer. It is important to note
291 that winter concentrations in the Rhine (main contributor to the IJsselmeer) have not changed much since the 1970s and
292 showing maximum concentrations of about $125 \mu\text{mol Si L}^{-1}$ in winter and clear seasonal dynamics due to uptake by diatoms
293 (unpublished results based on data provided by Pätsch (2024); available through [https://wiki.cen.uni-](https://wiki.cen.uni-hamburg.de/ifm/ECOHAM/DATA_RIVER)
294 [hamburg.de/ifm/ECOHAM/DATA_RIVER](https://wiki.cen.uni-hamburg.de/ifm/ECOHAM/DATA_RIVER)). We identified a silicate increase of $1.4 \mu\text{mol Si L}^{-1} \text{ h}^{-1}$ during ebb tide. Due to
295 the absence of large estuaries nearby and salinity consistently being above 32 at our tidal sampling station around the island
296 of Ameland, we exclude fresh water runoff as a major silicate source and indicate TA sources within the Wadden Sea.
297 Submarine groundwater discharge (SGD) was identified as a source for nutrient fluxes in tidal flat ecosystems in previous
298 studies (e.g., Billerbeck et al., 2006; Røy et al., 2008; Santos et al., 2021; Waska and Kim, 2011; Wu et al., 2013). Since we
299 observed relatively constant marine salinities, we suspect that deep pore water flow (e.g., Røy et al., 2008) enriched with
300 nutrients act as a source for our observed increasing TA and nutrients parameters. TA generation in tidal flats was also observed
301 by Faber et al. (2014), who focused on a large macro tidal embayment in southern Australia. They also found increasing TA
302 values during ebb tide, associated the TA increase with a higher fraction of pore water, and determined the tidal cycle as the
303 controlling force for pore water exchange. Their findings and the observed silicate outwash support our assumption that TA is
304 generated in the sediments of the tidal flats and is washed out during ebb tide. In addition, we exclude lateral advected signals
305 from more western regions as the Vlie Inlet, since the TA concentrations in the surface transect samples in the Vlie Inlet
306 (except of the two samples close to the coastal mainland near Harlingen) were in the same range as the other observed TA
307 concentrations and were smaller than the increasing TA concentrations during ebb tide. Both increases in TA and silicate are
308 tidal signals, and we identify TA generation in the sediments of the tidal flats here as the major local TA source.

309 **4.3.2 TA generating processes**

310 The observed TA generation of $7.6 \mu\text{mol TA kg}^{-1} \text{ h}^{-1}$ and the silicate increase of $1.4 \mu\text{mol Si L}^{-1} \text{ h}^{-1}$ indicated an excess of TA
311 (also Fig. 5b). A given TA:Si ratio of 2:1 (Marx et al. 2017) would account for a TA generation of $2.8 \mu\text{mol TA kg}^{-1} \text{ h}^{-1}$. High
312 Si concentrations in tidal flat pore water (Rutgers van der Loeff, 1974) and in situ production of Si from dissolving diatom
313 frustules are the most probable sources of the Si (e.g., van Bennekom et al., 1974). Since we observed more TA generated than
314 silicate being washed out, other biogeochemical processes must be responsible for the TA generation in the sediments of the
315 tidal flats in the Dutch Wadden Sea.

316

317 We exclude CaCO_3 dissolution as TA source in the overlying water, since the Ω values were clearly supersaturated with $\Omega >$
318 1 (Fig. 4h,i, Table B1). The continuous calcite supersaturation nicely indicated the inflow and dominance of North Sea water
319 during the flood, with Ω values similar to previously observed North Sea values ($\Omega \sim 3.5$ to 4) (Charalampopoulou et al.,
320 2011; Carter et al., 2014). In pore water, carbonate undersaturation and associated CaCO_3 dissolution can only be driven
321 metabolically, due to CO_2 production by OM remineralization, or due to the reoxidation of compounds reduced previously by
322 anaerobic processes (Brenner et al., 2016; Jahnke et al., 1994).

323

324 Other potential sources of TA generation in the sediments can be further narrowed down by a more detailed interpretation of
325 changes both in DIC (Δ DIC) and TA (Δ TA) during ebb tide, and their combination with various nutrient ratios. The correlation
326 of DIC and TA reveals an excess of released DIC compared to TA (Fig. 5a), as indicated by the slope of 1.87, while we
327 observed an increase in DIC (Δ DIC) almost twice as high as in TA (Δ TA). The high Δ DIC points to high aerobic OM
328 degradation and remineralization, resulting in high CO_2 production. High aerobic OM degradation was also previously
329 observed in the heterotrophic Wadden Sea (e.g., De Beer et al., 2005; van Beusekom et al., 1999), assuming an OM degradation
330 and remineralization occurring in the water and sediment in about equal parts (van Beusekom et al., 1999). High OM
331 degradation is indicated by the increasing $\text{C}_{\text{org}}:\text{N}$ ratios of SPM during ebb tide (Fig. 4k, Table B1). Because we observed
332 constant coastal North Sea salinities, we rule out fresh water runoff and terrestrial signals as source for the increasing $\text{C}_{\text{org}}:\text{N}$
333 ratios of SPM. We assume that fresh OM is rapidly degraded in the water column, and the older OM settles on and in the
334 sediment where the degradation continues and where it is resuspended at the low prevailing water levels during ebb. Therefore,
335 we assume that the increase of SPM concentrations and their $\text{C}_{\text{org}}:\text{N}$ ratios is an indicator for older and more refractory OM.
336 The increase in TA concentrations point to anaerobic processes, CaCO_3 dissolution, or a combination thereof as TA sources
337 occurring in the sediments.

338

339 For an upper bound estimate of sedimentary CaCO_3 dissolution as source of TA, we considered a DIC:TA ratio of 1:2.
340 Considering this ratio and the observed Δ TA of $51.6 \mu\text{mol TA kg}^{-1}$, CaCO_3 dissolution would lead to a potential Δ DIC of 25.8
341 $\mu\text{mol DIC kg}^{-1}$. The remaining potential $75.5 \mu\text{mol DIC kg}^{-1}$ ($101.3 - 25.8 \mu\text{mol DIC kg}^{-1}$) of the observed (Δ DIC) could then
342 be produced by OM degradation and remineralization, and would, using the expected Redfield ratio of C:N (6.6), correspond
343 to an estimated potential dissolved inorganic nitrogen (DIN) production of $11.4 \mu\text{mol DIN kg}^{-1}$. However, this estimated
344 potential DIN production ($11.4 \mu\text{mol DIN kg}^{-1}$) of OM degradation and remineralization exceeds the observed increase of
345 Δ DIN ($3.97 \mu\text{mol DIN L}^{-1}$; Table B1, sum of NO_3^- , NO_2^- and NH_4^+) during ebb tide. Based on this estimation and the
346 assumption that all DIN produced is released and thus lost, TA is probably produced by CaCO_3 dissolution and anaerobic
347 metabolic processes other than denitrification in the sediment. In addition to that, and with a N-focused perspective, the DIN
348 loss also hints to the occurrence of other processes that consume nitrogen species but have no net effect on TA, such as
349 anammox and coupled nitrification-denitrification (Hu and Cai, 2011; Middelburg et al., 2020). The suggested DIN loss can
350 be supported by considering the marine DIN:Si ratio, which is supposed to be about 1:1 (Brzezinski, 1985). We observed
351 DIN:Si ratios decreasing from 2.7 to 0.8 during ebb tide, showing that both parameter concentrations increased, whereby DIN
352 concentrations increased less than silicate concentrations. The silicate excess with respect to DIN at the end of ebb tide supports
353 the DIN loss.

354 Denitrification, the anaerobic irreversible reduction of NO_3^- to N_2 that generates 0.9 mole TA by using 1 mole NO_3^- as electron
355 acceptor (Chen and Wang, 1999) is a net TA source. Denitrification depends on the supply of nitrate, which seasonally varies
356 (van der Zee and Chou, 2005 and references therein). Generally, nitrate is depleted in summer due to high photosynthetic

357 activity and occurs in higher concentrations in winter (Kieskamp et al., 1991;Jensen et al., 1996;van der Zee and Chou, 2005).
358 This seasonality lead to denitrification rates also being lower in summer and higher in winter (Kieskamp et al., 1991;Jensen et
359 al., 1996). In previous studies, Faber et al. (2014) identified denitrification as a minor source of TA due to low denitrification
360 rates, and also Kieskamp et al. (1991) observed low denitrification rates in the Wadden Sea, with low nitrate concentrations
361 ($< 2.5 \mu\text{mol L}^{-1}$) in the overlying water. We observed nitrate concentrations ($< 2.17 \mu\text{mol L}^{-1}$) lower than the concentration
362 sufficient for denitrification assumed by Kieskamp et al. (1991). Therefore, we do not exclude denitrification, but suspect it as
363 a minor source of TA in the Dutch Wadden Sea at least in spring and summer due to the seasonal lack of nitrate. Thomas et
364 al. (2009) detected TA seasonality in the southern bight of the North Sea, which is also influenced by the TA generation in the
365 Wadden Sea. We support their findings of lowered TA generation by denitrification in late spring and early summer. In
366 addition, the calculated potential DIN excess compared to the observed DIN not only hints to other N consuming processes
367 that have no effect on TA, but also suggests that allochthonous nitrate would be needed to fuel the TA increase by
368 denitrification. In addition, the albeit low availability of nitrate indicates to predominantly aerobic metabolic activity in the
369 overlying water and upper sediment layers during the time of our observations, which is in line with earlier studies reporting
370 an enhanced relevance of anaerobic activity later in summer (Luff and Moll, 2004;Thomas et al., 2009).

371
372 The simultaneous increase of ammonium and TA (Fig. 4c, 4d, 5d) is important to notice, because under oxic conditions the
373 occurrence of ammonium is coupled with nitrification, a process that consumes ammonium and also TA (Chen and Wang,
374 1999). However, under anoxic conditions, such as in deeper sediment layers, ammonium cannot be reoxidized, accumulates,
375 and is washed out during ebb tide. Since we observed low nitrate concentrations and rule out terrestrial nitrate inputs here, the
376 increase in ammonium and TA implies the occurrence of other anaerobic processes of the redox system, such as sulfate and
377 iron reduction, to generate TA in the deeper, anoxic sediment layers in the Dutch Wadden Sea.

378 Sulfate reduction followed by iron reduction and the formation and burial of pyrite are net sources of TA, since TA
379 consumption by reoxidation is excluded when buried in sediments (Bernier et al., 1970;Faber et al., 2014). Whether these
380 processes contribute to TA generation in the deeper sediments of the Dutch Wadden Sea cannot be further identified without
381 the necessary data. However, sulfate reduction was also mentioned as source of TA by Thomas et al. (2009). The temporary
382 slight appearance of noticeable sulfuric odor could be another indirect indicator for the occurrence of sulfate reduction. In
383 previous studies of tidal flats in the German Wadden Sea, Beck et al. (2008a);(2008b) observed increasing TA concentrations
384 with depth and identified sulfate reduction as the most important process for anaerobic OM remineralization in pore water
385 cores.

386
387 A strict comparison of the northern and the western parts of the Wadden Sea is difficult because the areas vary in terms of OM
388 import and eutrophication effects (van Beusekom et al., 2019), sediment composition, and extent between the barrier islands
389 and the mainland, all of which influence the occurrence and interaction of biogeochemical processes (Schwichtenberg et al.,
390 2020). The area characteristics of the northern and western Wadden Sea differ especially in terms of OM turnover being lower

391 in the norther Wadden Sea. A previous study by Brasse et al. (1999) identified high TA and DIC concentrations in the sediment
392 of the North Frisian Wadden Sea and identified CaCO_3 dissolution and sulfate reduction as major TA sources, which is
393 consistent with our findings.

394 **5 Conclusion**

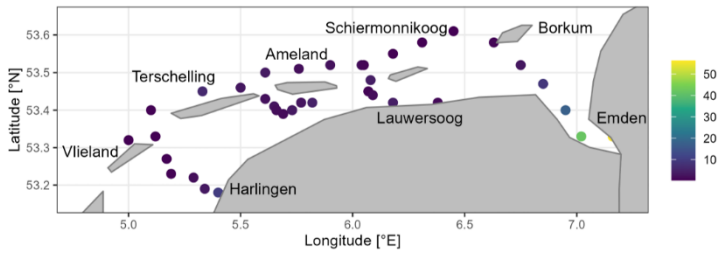
395 The Dutch Wadden Sea is a unique and highly dynamic ecosystem. We observed higher TA values in the Dutch Wadden Sea
396 than in the North Sea and identified the Dutch Wadden Sea as a TA source for the North Sea's carbonate system. Compared
397 to previous studies (Hoppema, 1990, 1993), the TA values we observed were in a similar range, with high TA values in the
398 tidal basins. Beside the need for seasonal observations, future work should also focus on regional and seasonal impacts of fresh
399 water inflows of TA on the TA status in the Dutch Wadden Sea.

400 By observing salinity and using dissolved silicate as a tracer, we excluded fresh water and river runoff as significant TA sources
401 on the tidal flats, and instead, deduced local outwash from the sediments as sources of TA. Considering various stoichiometries,
402 we suggest that CaCO_3 dissolution generates TA in the more upper oxic sediment layers, and anaerobic, metabolic processes
403 such as denitrification, sulfate and iron reduction are potential TA sources in the deeper anoxic sediment layers. However, in
404 spring and early summer, denitrification seems to play a minor role in generating TA in the sediments of the Dutch Wadden
405 Sea due to seasonality and associated limited nitrate availability.

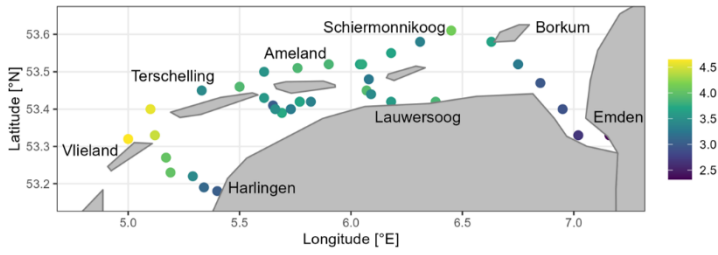
406 **6 Appendices**

407 **Appendix A**

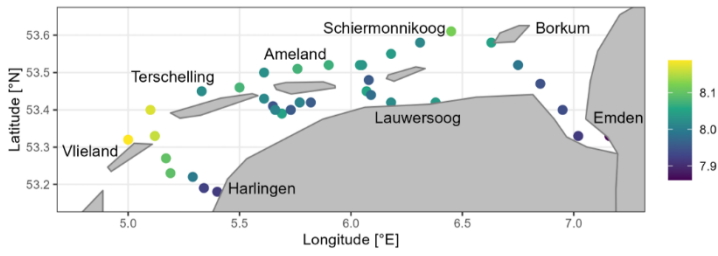
(A1a) Silicate ($\mu\text{ mol L}^{-1}$)



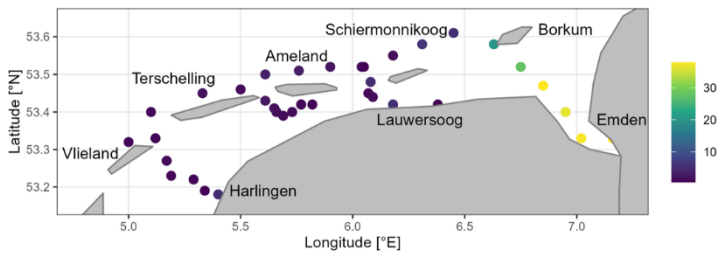
(A1b) Calcite saturation state (Ω)



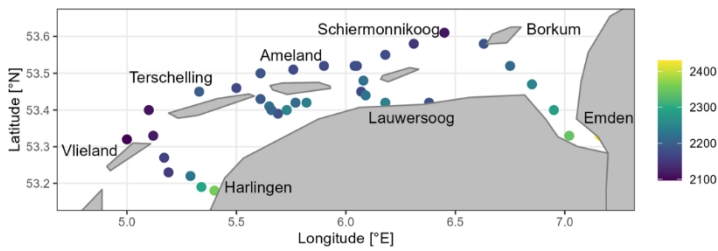
(A1c) pH



(A1d) Nitrate ($\mu\text{ mol L}^{-1}$)



(A1e) DIC ($\mu\text{ mol kg}^{-1}$)



409 **Figure A1** Spatial distribution of A1a) silicate (Si; $\mu\text{mol L}^{-1}$), A1b) calcite saturation state (Ω), A1c) pH, A1d) nitrate (NO_3^- ;
410 $\mu\text{mol L}^{-1}$), and A1e) dissolved inorganic carbon (DIC; $\mu\text{mol kg}^{-1}$) from surface water samples in May 2019.
411

412 **Appendix B**

413 **Table B1** Half tidal cycle sample parameter during ebb tide. Sample no. 545 is the first sample at high tide and sample no. 557
 414 is the last sample at low tide on 21 May 2019 (53.38°N & 5.62°E). Shown are rounded up values of temperature (Temp),
 415 salinity (Sal), total alkalinity (TA), dissolved inorganic carbon (DIC), silicate (Si), nitrate (NO₃⁻), nitrite (NO₂⁻), ammonium
 416 (NH₄⁺), dissolved inorganic nitrogen (DIN), the amount of carbon (C) and organic carbon (C_{org}) of SPM, the amount of nitrogen
 417 (N) of SPM, the calcite (Ca) and aragonite (Ar) saturation states, the pH, and phosphate (PO₄³⁻) per sample.

Sample No.	Time [UTC]	Temp [°C]	Sal	TA [μmol kg ⁻¹]	DIC [μmol kg ⁻¹]	Si [μmol L ⁻¹]	NO ₃ ⁻ [μmol L ⁻¹]	NO ₂ ⁻ [μmol L ⁻¹]	NH ₄ ⁺ [μmol L ⁻¹]
545	10:46	13.26	32.5	2387	2172	1.84	1.26	0.19	3.47
546	11:19	13.25	32.5	2385	2190	1.77	1.24	0.19	3.40
547	11:49	13.28	32.5	2389	2185	1.72	1.21	0.19	3.35
548	12:23	13.38	32.5	2391	2183	1.6	1.19	0.19	3.52
549	13:35	14.32	32.5	2400	2204	2.11	0.91	0.25	3.57
550	14:05	14.61	32.5	2400	2221	2.78	1.09	0.29	3.98
551	14:36	14.64	32.5	2405	2216	2.72	1.01	0.29	4.27
552	15:26	14.73	32.5	2411	2234	4.59	1.23	0.34	5.51
553	15:42	14.77	32.5	2402	2228	4.24	1.26	0.33	5.08
554	16:04	14.72	32.5	2419	2234	5.66	1.46	0.36	5.33
555	16:38	14.66	32.5	2428	2256	8.18	1.77	0.43	6.04
556	17:07	14.68	32.5	2433	2271	9.79	1.87	0.47	6.27
557	17:32	14.70	32.5	2438	2273	11.22	2.17	0.50	6.22
Sample No.	Time [UTC]	DIN [μmol L ⁻¹]	C / C _{org} (SPM) [μmol L ⁻¹]	N (SPM) [μmol L ⁻¹]	C _{org} :N (SPM)	SPM [mg L ⁻¹]	Ca / Ar [Ω]	pH	PO ₄ ³⁻ [μmol L ⁻¹]
545	10:46	4.93	86.8 / 65.1	8.8	7.4	12.8	3.8 / 2.4	8.07	0.12
546	11:19	4.83	72.7 / 42.4	7.4	5.8	8.7	3.5 / 2.3	8.03	0.11
547	11:49	4.76	112.4 / 93.4	9.6	9.7	15.4	3.7 / 2.3	8.05	0.11
548	12:23	4.91	108.5 / 104.6	9.9	10.5	16.8	3.7 / 2.4	8.05	0.12
549	13:35	4.73	111.1 / 97.8	8.8	11.1	13.9	3.6 / 2.3	8.01	0.32
550	14:05	5.37	233.0 / 180.3	17.7	10.2	32.2	3.3 / 2.1	7.97	0.42
551	14:36	5.56	193.2 / 174.3	14.5	12.0	29.6	3.5 / 2.2	7.99	0.47
552	15:26	7.08	248.6 / 163.5	18.4	8.9	34.3	3.3 / 2.1	7.96	0.57
553	15:42	6.67	257.6 / 199.3	18.3	10.9	41.6	3.2 / 2.1	7.95	0.54
554	16:04	7.15	324.4 / 271.1	23.2	11.7	55.0	3.4 / 2.2	7.98	0.54
555	16:38	8.24	440.4 / 345.2	29.2	11.8	75.7	3.2 / 2.1	7.95	0.58
556	17:07	8.61	430.5 / 363.3	27.9	13.0	82.4	3.1 / 2.0	7.93	0.62
557	17:32	8.90	308.9 / 199.1	21.2	9.4	48.8	3.1 / 2.0	7.93	0.63

418 **Table B2** Half tidal cycle sample parameter during high tide. Sample no. 564 is the first sample at low tide and sample no.
 419 578 is the last sample at high tide on 23 May 2019 (53.39°N & 5.63°E, 5.62°E*). Shown are rounded up values of temperature
 420 (Temp), salinity (Sal), total alkalinity (TA), dissolved inorganic carbon (DIC), silicate (Si), nitrate (NO₃⁻), nitrite (NO₂⁻),
 421 ammonium (NH₄⁺), dissolved inorganic nitrogen (DIN), the amount of carbon (C) and organic carbon (C_{org}) of SPM, the
 422 amount of nitrogen (N) of SPM, the calcite (Ca) and aragonite (Ar) saturation states, the pH, and phosphate (PO₄³⁻) per sample.

Sample No.	Time [UTC]	Temp [°C]	Sal	TA [μmol kg ⁻¹]	DIC [μmol kg ⁻¹]	Si [μmol L ⁻¹]	NO ₃ ⁻ [μmol L ⁻¹]	NO ₂ ⁻ [μmol L ⁻¹]	NH ₄ ⁺ [μmol L ⁻¹]
564	05:09	14.04	32.7	2431	2246	8.53	1.25	0.47	3.31
565	05:32	14.02	32.7	2441	2287	9.14	1.26	0.45	3.08
566	06:01	13.95	32.7	2436	2284	8.88	1.33	0.38	2.46
567	06:33	14.16	32.7	2443	2284	8.68	0.95	0.37	2.37
568	07:02	14.21	32.7	2432	2280	6.94	0.75	0.34	2.63
569	07:31	14.15	32.6	2401	2223	2.12	0.98	0.27	4.12
570	08:04	14.20	32.6	2403	2218	2.10	1.04	0.27	3.88
571	08:35	14.27	32.6	2409	2228	2.15	0.92	0.25	4.18
572	09:04	14.37	32.5	2400	2209	1.88	1.00	0.22	3.86
573	09:34	14.16	32.5	2398	2200	1.70	1.03	0.21	3.51
574*	10:02	14.17	32.5	2391	2197	1.72	1.07	0.21	3.40
575*	10:34	14.11	32.5	2389	2195	1.78	1.18	0.20	3.45
576	11:04	14.21	32.5	2390	2187	1.76	1.12	0.19	3.29
577	11:34	14.50	32.5	2399	2193	1.66	1.10	0.20	3.32
578	12:03	13.96	32.5	2390	2187	1.75	1.41	0.19	3.72
Sample No.	Time [UTC]	DIN [μmol L ⁻¹]	C / C _{org} (SPM) [μmol L ⁻¹]	N (SPM) [μmol L ⁻¹]	C _{org} :N (SPM)	SPM [mg L ⁻¹]	Ca / Ar [Ω]	pH	PO ₄ ³⁻ [μmol L ⁻¹]
564	05:09	5.03	353.7 / 253.2	27.5	9.2	52.3	3.04 / 2.2	7.99	0.38
565	05:32	4.78	333.5 / 220.1	26.1	8.4	49.7	3.0 / 1.9	7.92	0.37
566	06:01	4.17	330.3 / 232.9	25.5	9.1	51.7	2.9 / 1.9	7.91	0.34
567	06:33	3.68	274.7 / 195.7	21.8	9.0	36.9	3.0 / 1.9	7.92	0.33
568	07:02	3.72	317.8 / 220.2	24.5	9.0	46.1	2.9 / 1.9	7.91	0.32
569	07:31	5.37	88.6 / 59.1	7.0	8.5	14.7	3.3 / 2.1	7.98	0.33
570	08:04	5.20	96.8 / 73.6	8.8	8.4	18.1	3.4 / 2.2	7.99	0.30
571	08:35	5.35	114.2 / 109.6	9.9	11.0	14.8	3.3 / 2.1	7.98	0.32
572	09:04	5.08	107.5 / 73.9	9.9	7.5	16.4	3.5 / 2.2	8.00	0.26
573	09:34	4.75	82.1 / 72.7	7.2	10.0	11.8	3.6 / 2.3	8.02	0.21
574*	10:02	4.68	85.2 / 62.9	7.2	8.7	9.9	3.5 / 2.3	8.01	0.18
575*	10:34	4.83	83.5 / 65.9	7.2	9.2	11.1	3.5 / 2.3	8.01	0.16

576	11:04	4.60	82.7 / 52.1	8.2	6.3	8.5	3.7 / 2.3	8.03	0.14
577	11:34	4.62	65.8 / 50.8	6.5	7.8	7.2	3.7 / 2.4	8.03	0.16
578	12:03	5.32	71.6 / 54.6	7.7	7.1	7.7	3.7 / 2.3	8.04	0.11

423 **Data availability**

424 The data of this study are either presented in the article or are available upon request from the corresponding author.

425 **Author Contributions**

426 MN wrote the manuscript, did the carbon sampling and sample measurement, analyzed and evaluated the data, and led the
427 study. JvB led the research cruise. JvB and HT contributed with editorial and scientific recommendations. MN prepared the
428 manuscript with contribution from all co-authors.

429 **Competing interests**

430 The contact author has declared that none of the authors has any competing interests.

431 **Acknowledgement**

432 We thank the crew from RV *Ludwig Prandtl* for their support during the cruise. We thank Leon Schmidt for the nutrient
433 sampling and measurements, and Marc Metzke for the C/N measurements. We further thank the Editor and two anonymous
434 reviewers for their constructive comments, which greatly improved this manuscript.

435 **Financial support**

436 This research has been funded by the German Academic Exchange Service (DAAD, project: MOPGA-GRI, grant no.
437 57429828), which received funds from the German Federal Ministry of Education and Research (BMBF).

438 **References**

439 Abril, G., and Frankignoulle, M.: Nitrogen–alkalinity interactions in the highly polluted Scheldt basin (Belgium), *Water Research*, 35, 844-
440 850, [https://doi.org/10.1016/S0043-1354\(00\)00310-9](https://doi.org/10.1016/S0043-1354(00)00310-9), 2001.
441 Beck, M., Dellwig, O., Holstein, J. M., Grunwald, M., Liebezeit, G., Schnetger, B., and Brumsack, H.-J.: Sulphate, dissolved organic carbon,
442 nutrients and terminal metabolic products in deep pore waters of an intertidal flat, *Biogeochemistry*, 89, 221-238,
443 <https://doi.org/10.1007/s10533-008-9215-6>, 2008a.

444 Beck, M., Dellwig, O., Liebezeit, G., Schnetger, B., and Brumsack, H.-J.: Spatial and seasonal variations of sulphate, dissolved organic
445 carbon, and nutrients in deep pore waters of intertidal flat sediments, *Estuarine, Coastal and Shelf Science*, 79, 307-316,
446 <https://doi.org/10.1016/j.ecss.2008.04.007>, 2008b.

447 Berner, R. A., Scott, M. R., and Thomlinson, C.: Carbonate alkalinity in the pore waters of anoxic marine sediments I, *Limnology and*
448 *Oceanography*, 15, 544-549, <https://doi.org/10.4319/lo.1970.15.4.0544>, 1970.

449 Berner, R. A., Lasaga, A. C., and Garrels, R. M.: Carbonate-silicate geochemical cycle and its effect on atmospheric carbon dioxide over
450 the past 100 million years, *Am. J. Sci. (United States)*, 283, doi:10.2475/ajs.283.7.641., 1983.

451 Billerbeck, M., Werner, U., Polerecky, L., Walpersdorf, E., DeBeer, D., and Huettel, M.: Surficial and deep pore water circulation governs
452 spatial and temporal scales of nutrient recycling in intertidal sand flat sediment, *Marine Ecology Progress Series*, 326, 61-76, 2006.

453 Borges, A. V., Delille, B., and Frankignoulle, M.: Budgeting sinks and sources of CO₂ in the coastal ocean: Diversity of ecosystems counts,
454 *Geophysical research letters*, 32, doi.org/10.1029/2005GL023053, 2005.

455 Bozec, Y., Thomas, H., Elkalay, K., and de Baar, H. J.: The continental shelf pump for CO₂ in the North Sea—evidence from summer
456 observation, *Marine Chemistry*, 93, 131-147, <https://doi.org/10.1016/j.marchem.2004.07.006>, 2005.

457 Brasse, S., Reimer, A., Seifert, R., and Michaelis, W.: The influence of intertidal mudflats on the dissolved inorganic carbon and total
458 alkalinity distribution in the German Bight, southeastern North Sea, *Journal of Sea Research*, 42, 93-103, 1999.

459 Brenner, H., Braeckman, U., Le Guitton, M., and Meysman, F. J.: The impact of sedimentary alkalinity release on the water column CO₂
460 system in the North Sea, *Biogeosciences*, 13, 841-863, <https://doi.org/10.5194/bg-13-841-2016>, 2016.

461 Brewer, P. G., and Goldman, J. C.: Alkalinity changes generated by phytoplankton growth, *Limnology and Oceanography*, 21, 108-117,
462 <https://doi.org/10.4319/lo.1976.21.1.0108>, 1976.

463 Brzezinski, M. A.: The Si: C: N ratio of marine diatoms: interspecific variability and the effect of some environmental variables, *Journal of*
464 *Phycology*, 21, 347-357, <https://doi.org/10.1111/j.0022-3646.1985.00347.x>, 1985.

465 Burchard, H., Flöser, G., Staneva, J. V., Badewien, T. H., and Riethmüller, R.: Impact of density gradients on net sediment transport into
466 the Wadden Sea, *Journal of Physical Oceanography*, 38, 566-587, 2008.

467 Burt, W., Thomas, H., Hagens, M., Pätsch, J., Clargo, N., Salt, L., Winde, V., and Böttcher, M.: Carbon sources in the North Sea evaluated
468 by means of radium and stable carbon isotope tracers, *Limnology and Oceanography*, 61, 666-683, <https://doi.org/10.1002/lno.10243>, 2016.

469 Carter, B. R., Toggweiler, J., Key, R. M., and Sarmiento, J. L.: Processes determining the marine alkalinity and calcium carbonate saturation
470 state distributions, *Biogeosciences*, 11, 7349-7362, <https://doi.org/10.5194/bg-11-7349-2014>, 2014.

471 Charalampopoulou, A., Poulton, A. J., Tyrrell, T., and Lucas, M. I.: Irradiance and pH affect coccolithophore community composition on a
472 transect between the North Sea and the Arctic Ocean, *Marine Ecology Progress Series*, 431, 25-43, <https://doi.org/10.3354/meps09140>,
473 2011.

474 Chen, C. T. A., and Wang, S. L.: Carbon, alkalinity and nutrient budgets on the East China Sea continental shelf, *Journal of Geophysical*
475 *Research: Oceans*, 104, 20675-20686, <https://doi.org/10.1029/1999JC900055>, 1999.

476 Crutzen, P.: Geology of mankind, *Nature*, 415, <https://doi.org/10.1038/415023a>, 2002.

477 De Beer, D., Wenzhöfer, F., Ferdelman, T. G., Boehme, S. E., Huettel, M., van Beusekom, J. E., Böttcher, M. E., Musat, N., and Dubilier,
478 N.: Transport and mineralization rates in North Sea sandy intertidal sediments, Sylt-Rømø basin, Wadden Sea, *Limnology and*
479 *Oceanography*, 50, 113-127, 2005.

480 De Jonge, V., Essink, K., and Boddeke, R.: The Dutch Wadden Sea: a changed ecosystem, *Hydrobiologia*, 265, 45-71,
481 <https://doi.org/10.1007/BF00007262>, 1993.

482 Dickson, A., and Millero, F. J.: A comparison of the equilibrium constants for the dissociation of carbonic acid in seawater media, *Deep Sea*
483 *Research Part A. Oceanographic Research Papers*, 34, 1733-1743, [https://doi.org/10.1016/0198-0149\(87\)90021-5](https://doi.org/10.1016/0198-0149(87)90021-5), 1987.

484 Dickson, A. G.: An exact definition of total alkalinity and a procedure for the estimation of alkalinity and total inorganic carbon from titration
485 data, *Deep Sea Research Part A. Oceanographic Research Papers*, 28, 609-623, [https://doi.org/10.1016/0198-0149\(81\)90121-7](https://doi.org/10.1016/0198-0149(81)90121-7), 1981.

486 Duran-Matute, M., Gerkema, T., De Boer, G., Nauw, J., and Gräwe, U.: Residual circulation and freshwater transport in the Dutch Wadden
487 Sea: a numerical modelling study, *Ocean Science*, 10, 611-632, 2014.

488 Elias, E. P., Van der Spek, A. J., Wang, Z. B., and De Ronde, J.: Morphodynamic development and sediment budget of the Dutch Wadden
489 Sea over the last century, *Netherlands Journal of Geosciences*, 91, 293-310, <https://doi.org/10.1017/S0016774600000457>, 2012.

490 Faber, P. A., Evrard, V., Woodland, R. J., Cartwright, I. C., and Cook, P. L.: Pore-water exchange driven by tidal pumping causes alkalinity
491 export in two intertidal inlets, *Limnology and Oceanography*, 59, 1749-1763, <https://doi.org/10.4319/lo.2014.59.5.1749>, 2014.

492 Friedlingstein, P., O'sullivan, M., Jones, M. W., Andrew, R. M., Gregor, L., Hauck, J., Le Quéré, C., Luijckx, I. T., Olsen, A., and Peters, G.
493 P.: Global carbon budget 2022, *Earth System Science Data*, 14, 4811-4900, 2022.

494 Glavovic, B., Limburg, K., Liu, K., Emeis, K., Thomas, H., Kremer, H., Avril, B., Zhang, J., Mulholland, M., and Glaser, M.: Living on the
495 Margin in the Anthropocene: engagement arenas for sustainability research and action at the ocean-land interface, *Current Opinion in*
496 *Environmental Sustainability*, 14, 232-238, <https://doi.org/10.1016/j.cosust.2015.06.003>, 2015.

497 Grasshoff, K., Kremling, K., and Ehrhardt, M.: Methods of seawater analysis, John Wiley & Sons, 2009.

498 Hansen, H., and Koroleff, F.: Determination of nutrients. *Methods of Seawater Analysis: Third, Completely Revised and Extended Edition.*
499 Grasshoff, K., Kremling, K., and Ehrhardt, M. (Eds.), Weinheim, Germany: Wiley-VCH Verlag GmbH, 2007.

500 Hoppema, J.: The distribution and seasonal variation of alkalinity in the southern bight of the North Sea and in the western Wadden Sea,
501 Netherlands journal of sea research, 26, 11-23, [https://doi.org/10.1016/0077-7579\(90\)90053-J](https://doi.org/10.1016/0077-7579(90)90053-J), 1990.

502 Hoppema, J.: The oxygen budget of the western Wadden Sea, The Netherlands, Estuarine, Coastal and Shelf Science, 32, 483-502,
503 [https://doi.org/10.1016/0272-7714\(91\)90036-B](https://doi.org/10.1016/0272-7714(91)90036-B), 1991.

504 Hoppema, J.: Carbon dioxide and oxygen disequilibrium in a tidal basin (Dutch Wadden Sea), Netherlands journal of sea research, 31, 221-
505 229, [https://doi.org/10.1016/0077-7579\(93\)90023-L](https://doi.org/10.1016/0077-7579(93)90023-L), 1993.

506 Hu, X., and Cai, W. J.: An assessment of ocean margin anaerobic processes on oceanic alkalinity budget, Global Biogeochemical Cycles,
507 doi.org/10.1029/2010GB003859, 2011.

508 Huettel, M., Røy, H., Precht, E., and Ehrenhauss, S.: Hydrodynamical impact on biogeochemical processes in aquatic sediments, The
509 Interactions between Sediments and Water: Proceedings of the 9th International Symposium on the Interactions between Sediments and
510 Water, held 5–10 May 2002 in Banff, Alberta, Canada, 2003, 231-236,

511 Jahnke, R. A., Craven, D. B., and Gaillard, J.-F.: The influence of organic matter diagenesis on CaCO₃ dissolution at the deep-sea floor,
512 Geochimica et Cosmochimica Acta, 58, 2799-2809, 1994.

513 Jensen, K., Jensen, M., and Kristensen, E.: Nitrification and denitrification in Wadden Sea sediments (Königshafen, Island of Sylt, Germany)
514 as measured by nitrogen isotope pairing and isotope dilution, Aquatic Microbial Ecology, 11, 181-191, doi:10.3354/ame011181, 1996.

515 Keith, D. W., Ha-Duong, M., and Stolaroff, J. K.: Climate strategy with CO₂ capture from the air, Climatic Change, 74, 17-45,
516 <https://doi.org/10.1007/s10584-005-9026-x>, 2006.

517 Kérouel, R., and Aminot, A.: Fluorometric determination of ammonia in sea and estuarine waters by direct segmented flow analysis, Marine
518 Chemistry, 57, 265-275, [https://doi.org/10.1016/S0304-4203\(97\)00040-6](https://doi.org/10.1016/S0304-4203(97)00040-6), 1997.

519 Kieskamp, W. M., Lohse, L., Epping, E., and Helder, W.: Seasonal variation in denitrification rates and nitrous oxide fluxes in intertidal
520 sediments of the western Wadden Sea, Marine ecology progress series. Oldendorf, 72, 145-151, 1991.

521 Lewis, E., and Wallace, D.: Program developed for CO₂ system calculations, Environmental System Science Data Infrastructure for a Virtual
522 Ecosystem, 1998.

523 Louters, T., and Gerritsen, F.: The Riddle of the Sands: A Tidal System Vs Answer to a Rising Sea Level, report RIKZ-94.040 (isbn 90-369-
524 0084-0), 1994.

525 Luff, R., and Moll, A.: Seasonal dynamics of the North Sea sediments using a three-dimensional coupled sediment–water model system,
526 Continental Shelf Research, 24, 1099-1127, <https://doi.org/10.1016/j.csr.2004.03.010>, 2004.

527 Matthews, H. D., and Caldeira, K.: Stabilizing climate requires near-zero emissions, Geophysical research letters, 35,
528 <https://doi.org/10.1029/2007GL032388>, 2008.

529 Mehrbach, C., Culberson, C., Hawley, J., and Pytkowicz, R.: Measurement of the apparent dissociation constants of carbonic acid in seawater
530 at atmospheric pressure, Limnology and oceanography, 18, 897-907, <https://doi.org/10.4319/lo.1973.18.6.0897>, 1973.

531 Meybeck, M.: Global chemical weathering of surficial rocks estimated from river dissolved loads, American journal of science, 287, 401-
532 428, 10.2475/ajs.287.5.401, 1987.

533 Middelburg, J. J., Soetaert, K., and Hagens, M.: Ocean alkalinity, buffering and biogeochemical processes, Reviews of Geophysics, 58,
534 e2019RG000681, <https://doi.org/10.1029/2019RG000681>, 2020.

535 Norbistrath, M., Pätsch, J., Dähnke, K., Sanders, T., Schulz, G., van Beusekom, J. E., and Thomas, H.: Metabolic alkalinity release from
536 large port facilities (Hamburg, Germany) and impact on coastal carbon storage, Biogeosciences, 19, 5151-5165, <https://doi.org/10.5194/bg-19-5151-2022>, 2022.

537 Norbistrath, M., Neumann, A., Dähnke, K., Sanders, T., Schöl, A., van Beusekom, J. E., and Thomas, H.: Alkalinity and nitrate dynamics
538 reveal dominance of anammox in a hyper-turbid estuary, Biogeosciences, 20, 4307–4321, <https://doi.org/10.5194/bg-20-4307-2023>, 2023.

539 Pätsch, J.: Daily Loads of Nutrients, Total Alkalinity, Dissolved Inorganic Carbon and Dissolved Organic Carbon of the European
540 Continental Rivers for the Years 1977 – 2022. 2024.

541 Petersen, W., Schroeder, F., and Bockelmann, F.-D.: FerryBox-Application of continuous water quality observations along transects in the
542 North Sea, Ocean Dynamics, 61, 1541-1554, <https://doi.org/10.1007/s10236-011-0445-0>, 2011.

543 Postma, H.: Hydrography of the Dutch Wadden sea, Arch. Neerl. Zool, 10, 405-511, 1954.

544 Renforth, P., and Henderson, G.: Assessing ocean alkalinity for carbon sequestration, Reviews of Geophysics, 55, 636-674,
545 <https://doi.org/10.1002/2016RG000533>, 2017.

546 Ridderinkhof, H., Zimmerman, J., and Philippart, M.: Tidal exchange between the North Sea and Dutch Wadden Sea and mixing time scales
547 of the tidal basins, Netherlands Journal of Sea Research, 25, 331-350, [https://doi.org/10.1016/0077-7579\(90\)90042-F](https://doi.org/10.1016/0077-7579(90)90042-F), 1990.

548 Røy, H., Lee, J. S., Jansen, S., and de Beer, D.: Tide-driven deep pore-water flow in intertidal sand flats, Limnology and oceanography, 53,
549 1521-1530, <https://doi.org/10.4319/lo.2008.53.4.1521>, 2008.

550 Rutgers van der Loeff, M.: Transport van reactief silikaat uit Waddenzee sediment naar het bovenstaande water, NIOZ-rapport, 1974.

551 Sabine, C. L., Feely, R. A., Gruber, N., Key, R. M., Lee, K., Bullister, J. L., Wanninkhof, R., Wong, C., Wallace, D. W., and Tilbrook, B.:
552 The oceanic sink for anthropogenic CO₂, science, 305, 367-371, DOI: 10.1126/science.1097403, 2004.

554 Santos, I. R., Chen, X., Lecher, A. L., Sawyer, A. H., Moosdorf, N., Rodellas, V., Tamborski, J., Cho, H.-M., Dimova, N., and Sugimoto,
555 R.: Submarine groundwater discharge impacts on coastal nutrient biogeochemistry, *Nature Reviews Earth & Environment*, 2, 307-323,
556 <https://doi.org/10.1038/s43017-021-00152-0>, 2021.

557 Schwichtenberg, F., Callies, U., and van Beusekom, J. E.: Residence times in shallow waters help explain regional differences in Wadden
558 Sea eutrophication, *Geo-Marine Letters*, 37, 171-177, <https://doi.org/10.1007/s00367-016-0482-2>, 2017.

559 Schwichtenberg, F., Pätsch, J., Böttcher, M. E., Thomas, H., Winde, V., and Emeis, K.-C.: The impact of intertidal areas on the carbonate
560 system of the southern North Sea, *Biogeosciences*, 17, 4223-4245, <https://doi.org/10.5194/bg-17-4223-2020>, 2020.

561 Shadwick, E., Thomas, H., Gratton, Y., Leong, D., Moore, S., Papakyriakou, T., and Prowe, A.: Export of Pacific carbon through the Arctic
562 Archipelago to the North Atlantic, *Continental Shelf Research*, 31, 806-816, <https://doi.org/10.1016/j.csr.2011.01.014>, 2011.

563 Suchet, P. A., and Probst, J.-L.: Modelling of atmospheric CO₂ consumption by chemical weathering of rocks: application to the Garonne,
564 Congo and Amazon basins, *Chemical Geology*, 107, 205-210, DOI:10.1016/0009-2541(93)90174-H, 1993.

565 Thomas, H., Bozec, Y., Elkalay, K., and De Baar, H. J.: Enhanced open ocean storage of CO₂ from shelf sea pumping, *Science*, 304, 1005-
566 1008, DOI: 10.1126/science.1095491, 2004.

567 Thomas, H., Schiettecatte, L.-S., Suykens, K., Koné, Y., Shadwick, E., Prowe, A. F., Bozec, Y., de Baar, H. J., and Borges, A.: Enhanced
568 ocean carbon storage from anaerobic alkalinity generation in coastal sediments, *Biogeosciences*, 6, 267-274, [https://doi.org/10.5194/bg-6-](https://doi.org/10.5194/bg-6-267-2009)
569 [267-2009](https://doi.org/10.5194/bg-6-267-2009), 2009.

570 van Bennekom, A., Krijgsman-van Hartingsveld, E., van der Veer, G., and van Voorst, H.: The seasonal cycles of reactive silicate and
571 suspended diatoms in the Dutch Wadden Sea, *Netherlands Journal of Sea Research*, 8, 174-207, [https://doi.org/10.1016/0077-](https://doi.org/10.1016/0077-7579(74)90016-7)
572 [7579\(74\)90016-7](https://doi.org/10.1016/0077-7579(74)90016-7), 1974.

573 van Beusekom, J., Brockmann, U., Hesse, K.-J., Hickel, W., Poremba, K., and Tillmann, U.: The importance of sediments in the
574 transformation and turnover of nutrients and organic matter in the Wadden Sea and German Bight, *Deutsche Hydrografische Zeitschrift*, 51,
575 245-266, 10.1007/BF02764176, 1999.

576 van Beusekom, J., and De Jonge, V.: Long-term changes in Wadden Sea nutrient cycles: importance of organic matter import from the North
577 Sea, in: *Nutrients and Eutrophication in Estuaries and Coastal Waters*, Springer, 185-194, 2002.

578 van Beusekom, J. E., Buschbaum, C., and Reise, K.: Wadden Sea tidal basins and the mediating role of the North Sea in ecological processes:
579 scaling up of management?, *Ocean & coastal management*, 68, 69-78, <https://doi.org/10.1016/j.ocecoaman.2012.05.002>, 2012.

580 van Beusekom, J. E., Carstensen, J., Dolch, T., Grage, A., Hofmeister, R., Lenhart, H., Kerimoglu, O., Kolbe, K., Pätsch, J., and Rick, J.:
581 Wadden Sea Eutrophication: long-term trends and regional differences, *Frontiers in Marine Science*, 6, 370,
582 doi.org/10.3389/fmars.2019.00370, 2019.

583 van der Zee, C., and Chou, L.: Seasonal cycling of phosphorus in the Southern Bight of the North Sea, *Biogeosciences*, 2, 27-42,
584 <https://doi.org/10.5194/bg-2-27-2005>, 2005.

585 van Raaphorst, W., and van der Veer, H. W.: The phosphorus budget of the Marsdiep tidal basin (Dutch Wadden Sea) in the period 1950-
586 1985: importance of the exchange with the North Sea, in: *North Sea—Estuaries Interactions*, Springer, 21-38, 1990.

587 Voynova, Y. G., Petersen, W., Gehrung, M., Aßmann, S., and King, A. L.: Intertidal regions changing coastal alkalinity: The Wadden Sea-
588 North Sea tidally coupled bioreactor, *Limnology and Oceanography*, 64, 1135-1149, 2019.

589 Wang, Z. A., Kroeger, K. D., Ganju, N. K., Gonnee, M. E., and Chu, S. N.: Intertidal salt marshes as an important source of inorganic
590 carbon to the coastal ocean, *Limnology and Oceanography*, 61, 1916-1931, 2016.

591 Waska, H., and Kim, G.: Submarine groundwater discharge (SGD) as a main nutrient source for benthic and water-column primary
592 production in a large intertidal environment of the Yellow Sea, *Journal of Sea Research*, 65, 103-113,
593 <https://doi.org/10.1016/j.seares.2010.08.001>, 2011.

594 Wolf-Gladrow, D. A., Zeebe, R. E., Klaas, C., Körtzinger, A., and Dickson, A. G.: Total alkalinity: The explicit conservative expression and
595 its application to biogeochemical processes, *Marine Chemistry*, 106, 287-300, <https://doi.org/10.1016/j.marchem.2007.01.006>, 2007.

596 Wu, Z., Zhou, H., Zhang, S., and Liu, Y.: Using ²²²Rn to estimate submarine groundwater discharge (SGD) and the associated nutrient fluxes
597 into Xiangshan Bay, East China Sea, *Marine pollution bulletin*, 73, 183-191, <https://doi.org/10.1016/j.marpolbul.2013.05.024>, 2013.

598 Zalasiewicz, J., Williams, M., Steffen, W., and Crutzen, P.: *The new world of the Anthropocene*. ACS Publications, 2010.

599 Zhang, C., Shi, T., Liu, J., He, Z., Thomas, H., Dong, H., Rinkevich, B., Wang, Y., Hyun, J.-H., and Weinbauer, M.: Eco-engineering
600 approaches for ocean negative carbon emission, *Science Bulletin*, 67, 2564-2573, <https://doi.org/10.1016/j.scib.2022.11.016>, 2022.

601